

# Graphene-Based Standalone Solar Energy Converter for Water Desalination and Purification

Yang Yang,<sup>†,‡</sup> Ruiqi Zhao,<sup>†,‡</sup> Tengfei Zhang,<sup>†,‡</sup> Kai Zhao,<sup>†,‡</sup> Peishuang Xiao,<sup>†,‡</sup> Yanfeng Ma,<sup>†,‡</sup> Pulickel M. Ajayan,<sup>§</sup> Gaoquan Shi,<sup>⊥</sup> and Yongsheng Chen<sup>\*,†,‡,Ⓜ</sup>

<sup>†</sup>The Centre of Nanoscale Science and Technology and Key Laboratory of Functional Polymer Materials, State Key Laboratory and Institute of Elemento-Organic Chemistry, College of Chemistry, and <sup>‡</sup>The National Institute for Advanced Materials, Nankai University, Tianjin 300071, China

<sup>§</sup>Department of Materials Science and Nano Engineering, Rice University, Houston, Texas 77005, United States

<sup>⊥</sup>Department of Chemistry, Tsinghua University, Beijing 100084, China

## S Supporting Information

**ABSTRACT:** Harvesting solar energy for desalination and sewage treatment has been considered as a promising solution to produce clean water. However, state-of-the-art technologies often require optical concentrators and complicated systems with multiple components, leading to poor efficiency and high cost. Here, we demonstrate an extremely simple and standalone solar energy converter consisting of only an as-prepared 3D cross-linked honeycomb graphene foam material without any other supporting components. This simple all-in-one material can act as an ideal solar thermal converter capable of capturing and converting sunlight into heat, which in turn can distill water from various water sources into steam and produce purified water under ambient conditions and low solar flux with very high efficiency. High specific water production rate of  $2.6 \text{ kg h}^{-1} \text{ m}^{-2} \text{ g}^{-1}$  was achieved with near  $\sim 87\%$  under 1 sun intensity and  $>80\%$  efficiency even under ambient sunlight ( $<1$  sun). This scalable sheet-like material was used to obtain pure drinkable water from both seawater and sewage water under ambient conditions. Our results demonstrate a competent monolithic material platform providing a paradigm change in water purification by using a simple, point of use, reusable, and low-cost solar thermal water purification system for a variety of environmental conditions.



**KEYWORDS:** solar energy conversion, water desalination and purification, graphene, standalone, all-in-one

Solar energy is the truly original and eventual source of all energy on earth.<sup>1,2</sup> As the most abundant and sustainable source of renewable and clean energy, solar energy can be used in many processes, such as photovoltaics,<sup>3,4</sup> photocatalysis,<sup>5,6</sup> and solar thermal conversion.<sup>7–9</sup> For the solar thermal conversion, harvesting solar energy as heat has played an important role for many applications, such as power generation, residential water heating, desalination, and sewage treatment.<sup>1</sup> In this regard, while much progress and many approaches have been made, most of them still exhibit the challenge to achieve higher efficiency, improved scalability, and lower cost with simpler structure.<sup>7–13</sup> On the other side, a sanitary and clean water source has been the main limiting issue in many regions and situations both strategically and tactically.<sup>14,15</sup> The most important approaches to increase water supply beyond what is available from the hydrological cycle are desalination and sewage treatment.<sup>15</sup> One of such platforms to supply the fresh water is using seawater reverse osmosis (SWRO) technology,<sup>15–20</sup> which runs under the energy cost of

$\sim 3 \text{ kWh m}^{-3}$  and emits  $\sim 1.4 \text{ kg CO}_2$  per cubic meter of produced water.<sup>15</sup> Furthermore, SWRO also needs pretreatment of a water source and cannot treat high-salinity water.<sup>15,21</sup>

With these, it would be ideal to develop disruptive technologies to have clean water access with both high efficiency and low cost and best by using natural sunlight directly.<sup>15</sup> For this goal, the key is to develop material/setup that can absorb and convert sunlight efficiently with both low cost and easy scalability.<sup>7</sup> Indeed, tremendous effort and progress have been made<sup>7–13,22,23</sup> in this area. Most recently, metallic nanoparticles, such as gold,<sup>24–27</sup> alumina,<sup>9</sup> and other nanoparticles,<sup>23,28–32</sup> have been proposed for steam and clean water generation under solar irradiation. However, the high cost, complicated fabrication process, and potential safety issue

Received: November 18, 2017

Accepted: January 4, 2018

Published: January 4, 2018

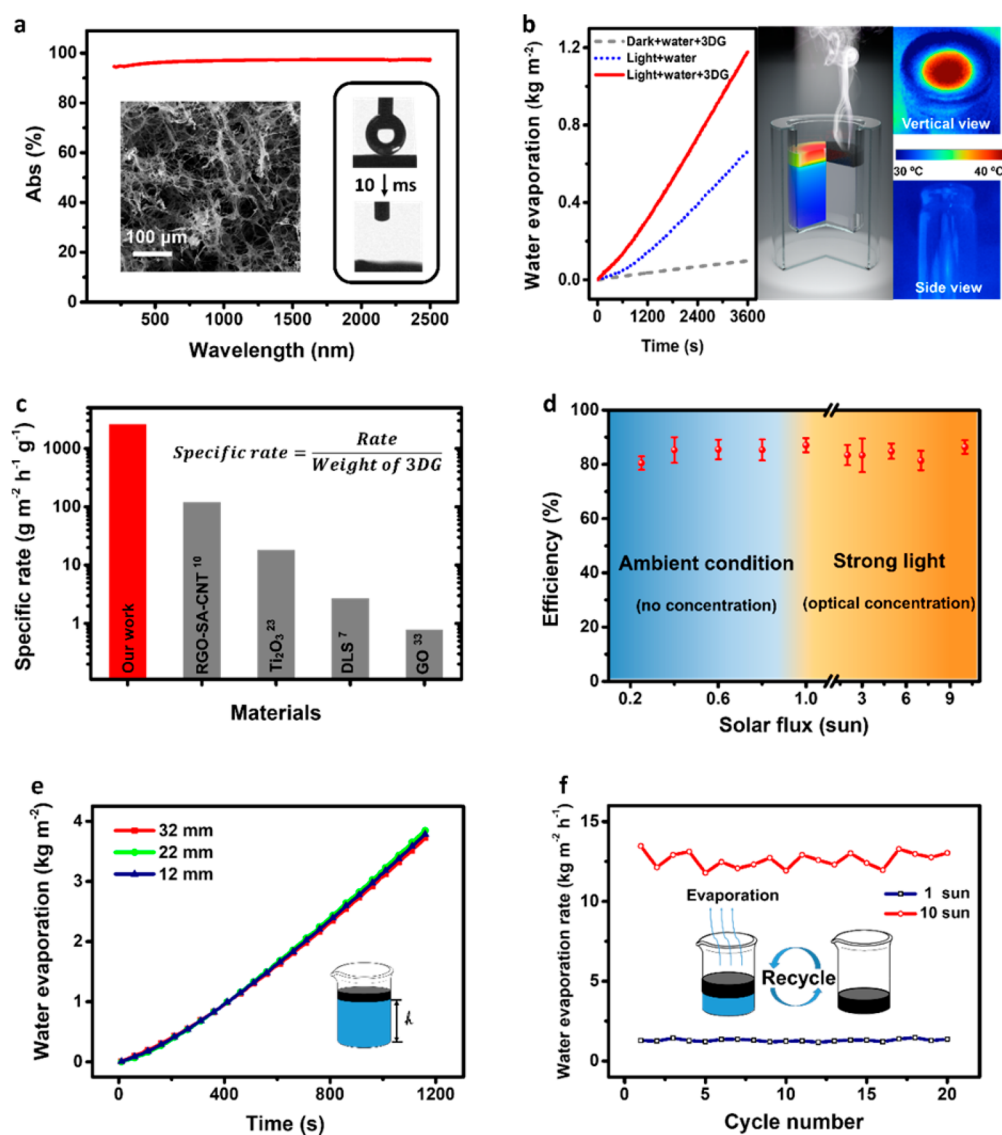


**Figure 1.** Solar thermal performance of the 3D graphene material. (a) Absorption spectrum of 3DG. It shows a blackbody-like property with  $\sim 97\%$  absorption across 200–2500 nm. Left part of the inset is the SEM image showing its porous morphology. Such morphology benefits from efficient light absorption through the multiscattering effect and water transportation through the interconnected pores. Right part of the inset is the contact angle showing it is superhydrophilic. (b) Left is the evaporation mass of water with/without 3DG under  $1 \text{ kW m}^{-2}$  solar irradiation and the case without light; the middle is the schematic illustration of 3DG for the vapor generation and the temperature distribution (cross section); the right part is the IR image of vertical and side view under  $1 \text{ kW m}^{-2}$ . The sample is smaller than the water/air interface to show that such a material can effectively prevent the heat conduction surrounding water. (c) Specific water production rate (water production rate/weight of 3DG) compared with some highest performing bulk converters reported in literature. (d) Solar thermal efficiency of the evaporation process by the 3DG under a range of optical concentrations. Error bars represent standard deviation for the same repeated measurements. (e) Performance of the 3DG with different water quantities under  $10 \text{ kW m}^{-2}$ . The device was in the same diameter but different heights of water at 32 mm (red), 22 mm (green), and 12 mm (blue). (f) Reusability of 3DG under 1 and  $10 \text{ kW m}^{-2}$  solar irradiation for 20 cycles with a NaCl solution, mimicking the seawater. Each cycle was tested for 2 h.

have been limiting their possible practical applications.<sup>21</sup> Thus, in recent years, carbon materials have attracted much interest, partially due to their low cost and efficient broadband absorption, which are the most important requirements to enable efficient solar thermal conversion and water purification applications in practice.<sup>7,8,10,21,33–39</sup> For instance, Chen's group has developed a double-layer structure (exfoliated graphite and porous carbon foam) for steam generation.<sup>7</sup> Zhu and co-workers also reported a GO-SA-CNT aerogel<sup>10</sup> and GO film with 2D water path<sup>33</sup> for high-efficiency steam generation and desalination. Hu's group developed a 3D printing fabrication technique using GO and CNT for solar energy harvesting for

high-efficiency steam generation.<sup>34</sup> However, to achieve high efficiency, almost all the current designs or systems require costly optical concentrators and complicated systems with multiple components including extra supporting part or insulating layer. These thus have been limiting their both scalability and feasibility.<sup>7,13,21,32–35</sup>

Previously, a 3D cross-linked polymer-like graphene material (3DGraphene), obtained from graphene oxide (GO) in large scale, has demonstrated many excellent properties based on graphene due to its multidimensional/scale nano/micro-structure,<sup>40–43</sup> such as superelasticity<sup>40</sup> and ammonia synthesis under ambient conditions.<sup>6</sup> Herein, we demonstrate an innately

one-component, standalone solar thermal converter, made directly from an as-prepared graphene-based 3D cross-linked polymer-like graphene material (3DG), with an extremely high specific water production rate of  $2.6 \text{ kg h}^{-1} \text{ m}^{-2} \text{ g}^{-1}$  and 87% energy efficiency under 1 sun solar radiation. More importantly, using this simple ready-to-go material device, the solar thermal conversion can achieve over 80% efficiency under a range of solar flux especially ambient sunlight (from 0.25 to 1 sun, conforming to the real outside condition). The high efficiency is achieved due to the combination of multiple properties simultaneously exhibited by this as-prepared bulk 3D cross-linked honeycomb graphene material, including its intrinsic blackbody-like high absorption, extremely low thermal loss to environment, hydrophilicity, and automatic water transportation to the absorber by capillary force through the microchannels present in the structure. With these results, an efficient and scalable desalination (4 orders of salinity decrement) and sewage treatment device was demonstrated. A model for this converter has been used to understand the high efficiency and mechanism.

## RESULT AND DISCUSSION

**Material Structure and Properties.** The as-prepared sheet-like, porous bulk graphene material (details in [Experimental Section](#)) can be used as a sunlight capture and conversion device directly without any additional component. Furthermore, this material could be made in large scale using a simple and industrial solvothermal method<sup>40–43</sup> and entirely consists of graphene sheets as 2D atomic layer building blocks cross-linked together mainly at the edge with a honeycomb-like porous structure and >99.9% porosity.<sup>40–43</sup> Thus, it is actually a monolithic and highly porous graphene-based material. This morphology makes it exhibit extremely low density ( $\sim 1 \text{ mg cm}^{-3}$ ), a high specific surface area of  $218 \text{ m}^2 \text{ g}^{-1}$  ([Figure S1](#)), and a low thermal conductivity (dry state:  $0.016 \text{ W m}^{-1} \text{ K}^{-1}$ , wet state:  $0.45 \text{ W m}^{-1} \text{ K}^{-1}$ ; details in [Supporting Information](#)),<sup>40</sup> so that it could float on water alone without any other structural support or thermal insulator attached.

The material shows a blackbody-like property with  $\sim 97\%$  absorption across 200–2500 nm ([Figure 1a](#)), benefiting from both the intrinsic absorption properties of graphene and its honeycomb structure (left inset of [Figure 1a](#) and [Figure S2](#)) with multiscattering effect.<sup>43</sup> The high hydrophilicity (right inset in [Figure 1](#)) and automatic water transportation into the absorber *via* capillary force through the microchannels could ensure an efficient water supply during the water vapor generation. Thus, this material exhibits in nature the much desired and multiple characteristics<sup>7</sup> simultaneously required for an ideal sunlight capture and conversion process, including its blackbody-like absorption, extremely low thermal loss to the environment, hydrophilicity, and automatic water transportation to the absorber by capillary force through the microchannel.

**High Solar Thermal Performance under Sunlight Illumination.** With these, the solar thermal conversion performance was evaluated for the material by simply placing (floating) a piece of this material on water directly (detailed in [Experimental Section](#)). Note that due to its low density and high hydrophilicity, the material can float on the water and be saturated with water automatically without any further fabrication or supporting part ([Figure S3](#)). The water vapor gets generated immediately once the light is incident on the

material ([Movie S1](#)), and the water evaporation over time with 3DG was measured by a real-time balance ([Figure S3](#)).

The typical curves of time-dependent water evaporation under 1 sun are provided in [Figure 1b](#) for a sample with a thickness of  $500 \mu\text{m}$  ( $0.10 \text{ mg}$ ,  $1.77 \text{ cm}^2$ ), and the evaporation rates were calculated from the slope of the curves. With this material, the water evaporation rate reaches  $1.30 \text{ kg m}^{-2} \text{ h}^{-1}$  (calculated from the slope of the curves, and the rate of water evaporation under the dark environment is subtracted), more than double ( $0.59 \text{ kg m}^{-2} \text{ h}^{-1}$ ) without this material on water. Importantly, the specific water production rate per absorber weight (rate/weight), a more practical indicator for the real application, is as high as  $2.6 \text{ kg m}^{-2} \text{ h}^{-1} \text{ g}^{-1}$ , more than 1 order higher than that of the highest performing bulk converters reported in literature, as shown in [Figure 1c](#).<sup>7,10,23,33</sup> The water evaporation rates of 3DG with different size ([Figure S4](#)) and humidity ([Figure S5](#)) under 1 sun were also carried out.

The energy conversion efficiency ( $\eta$ ) is defined as  $\eta = \dot{m}h_{\text{fg}}/Aq_{\text{solar}}$ , where  $\dot{m}$  denotes the water evaporation rate (the rate of water evaporation under the dark environment is subtracted),  $h_{\text{fg}}$  is the enthalpy of the liquid–vapor phase change,  $A$  is the surface area of the absorber facing the sun, and  $q_{\text{solar}}$  is the power density of solar illumination.<sup>8</sup> Under 1 sun illumination, the efficiency of 3DG can achieve  $87.04 \pm 2.61\%$ , superior to most of the previous reports,<sup>7–9,21,33–36</sup> as detailed in [Table S1](#). Furthermore, this material can also work well with a high efficiency in a wide range of sunlight intensities, particularly under the situation of ambient/natural sunlight with low solar flux. As shown in [Figure 1d](#), the energy efficiency is greater than >80% under different low solar fluxes (<1 sun), even down to 0.25 sun. These results carry more significance for real industry application as no costly and complicated optical concentration equipment is required to achieve high efficiency and water production under ambient sunlight flux. The heat localization caused by the 3DG was investigated using an infrared camera and a temperature probe to monitor the temperature on vertical and side view, as shown in [Figure 1b](#). After 1 h illumination, the surface temperature of the 3DG (measured by temperature probe, shown in [Figure S6](#)) was up to above  $40 \text{ }^\circ\text{C}$ . However, water temperature around and underlying the 3DG was still maintained around  $30 \text{ }^\circ\text{C}$ , indicating little heat loss due to its low thermal conductivity.

### Independence of Water Quantity and in Bulk Water.

To more closely mimic the realistic situation where bulk amounts of water is used, a series of experiments with different quantities of water under 10 sun were carried out. As shown in [Figure 1e](#), with increased water quantity, from 12 to 32 mm for its height, the water evaporation rates remain almost unchanged. On the contrary, the rate without the 3DG decreased significantly with the increased water quantity ([Figure S7](#)), owing to the heat loss to bulk water. This indicates that the 3DG can be used efficiently with different scales and water quantities, important for large-scale application.

**Reusability.** To characterize the reusability of our 3DG, we prepared saline water with 3.5 wt % NaCl to mimic the seawater and also performed the solar water evaporation experiment repeatedly using the same sample. As shown in [Figure 1f](#), the evaporation rates of 20 cycles in saline water were stable under 1 and even high 10 sun illumination, demonstrating the reusability of the 3DG. During each cycle, the water was evaporated and 3DG shrank with salt deposition on the sample surface. After adding the salt water again, the

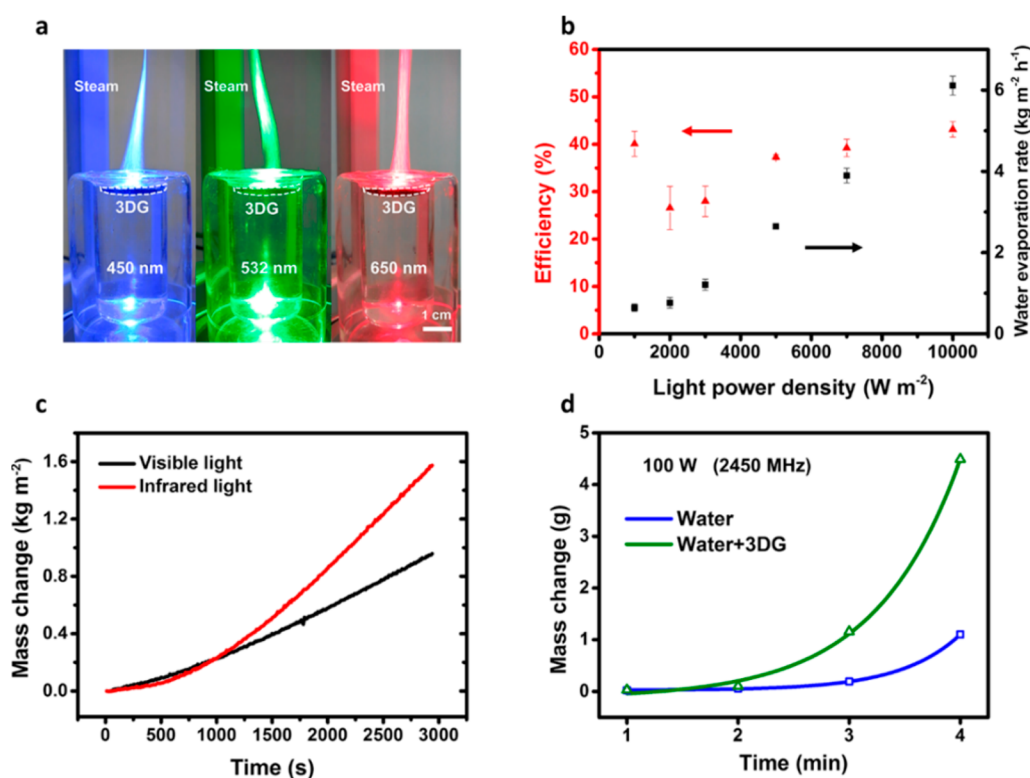


Figure 2. Solar thermal performance of 3DG in different wavelength ranges. (a) Optical images of vapor generation under different wavelengths (450, 532, and 650 nm) of the visible light. (b) Efficiency (left-hand side axis) and corresponding water evaporation rate (right-hand side axis) under different optical concentrations with wavelength of the 650 nm monochromatic light. Error bars represent standard deviation for the same repeated measurements. (c) Evaporation mass loss of water with 3DG under 1 sun solar irradiation of visible and infrared light. (d) Evaporation mass loss of water with 3DG under 100 W microwave (2450 MHz).

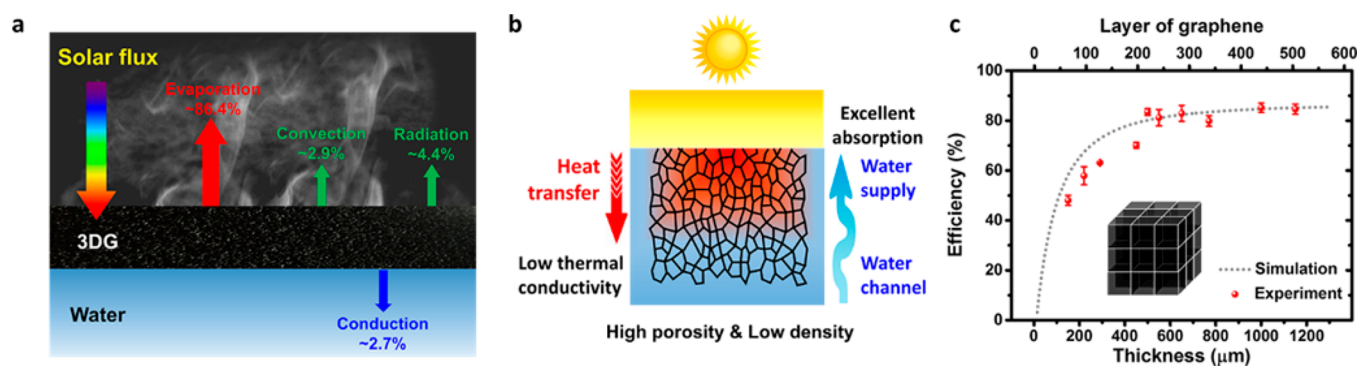
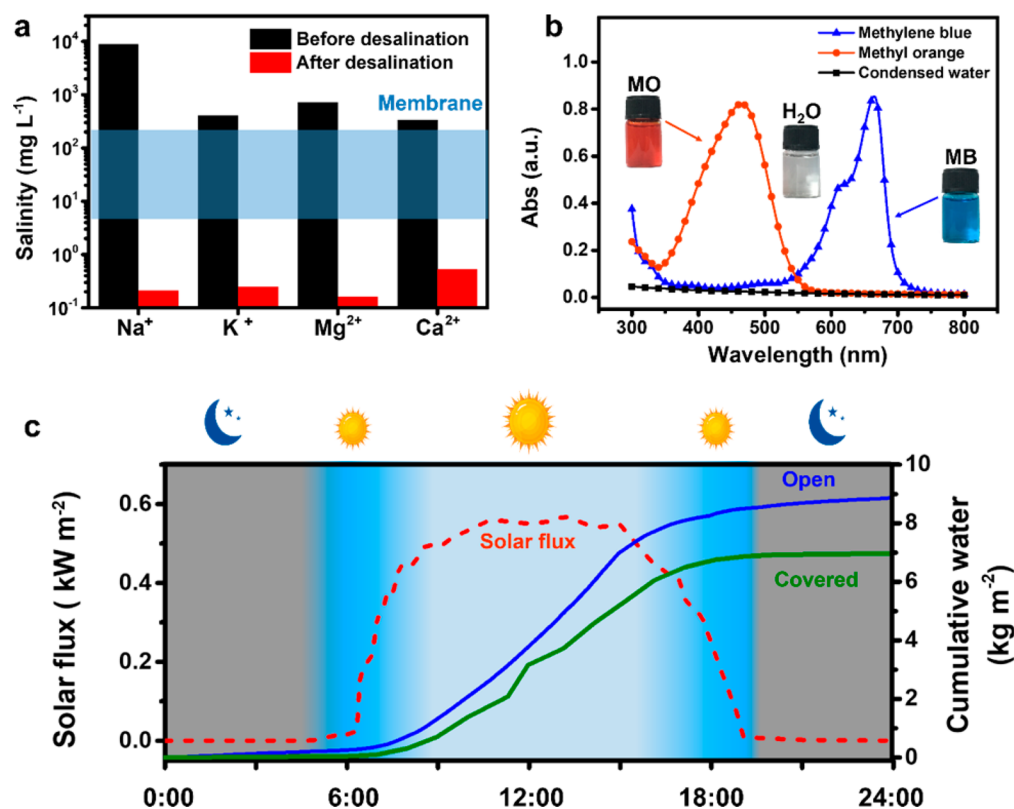


Figure 3. Mechanism and modeling for high performance. (a) Energy balance and heat transfer diagram in 3DG architecture during vapor generation process. (b) Zoomed-in diagram for the thermal environment of the 3DG during vapor generation process. (c) Experimental vapor generation efficiency vs different thickness of the 3DG (simulated layers of graphene). The predicted efficiency profile is also included in (c), showing good agreement with experimental results. Error bars represent standard deviation for the same repeated measurements.

deposited salt dissolved, and the 3DG recovered to its initial shape floating on the water surface and was ready for the next cycle. The structure of the material after 20 cycles was characterized, showing that the structure barely changed in spite of the NaCl crystal continuously depositing on the graphene sheet (Figure S8). These results also indicate that the performance is not impacted by the salt concentration (see Supporting Information). Meanwhile, a long-time test over 5 h with a large amount of bulk water was also carried out (Figure S9), and the rate remained nearly unchanged. Note, such a 3DG material also has a highly reversible elasticity (Figures S10 and S11)<sup>40</sup> and can be packed/squeezed to a real small volume for a long time for storage and then used directly and

repeatedly. Considering its excellent dry and wet strength as well as the thermo-mechanical stability, it is particularly attractive for long-term and harsh/remote environment solar desalination and sanitary water production application.

**Performance under Different Wavelengths.** For the effect of light with different wavelengths, the solar thermal performance of 3DG in different wavelength ranges including monochromatic light was systematically investigated. Optical images of vapor generation under different monochromatic lights (450, 532, and 650 nm) are shown in Figure 2a (Movie S2). The efficiencies and corresponding rates under a typical wavelength (650 nm) with different light intensities are shown in Figure 2b, and the performance of other wavelengths of



**Figure 4.** Clean water generation and outdoor performance under natural sunlight. (a) Salinities (the weight percentage of ions) of Na<sup>+</sup>, K<sup>+</sup>, Mg<sup>2+</sup>, and Ca<sup>2+</sup> before and after desalination. After the desalination, the concentration is below the values obtained through membrane-based seawater desalination (10–500 mg L<sup>-1</sup>). (b) Sewage treatment performance by 3DG under solar illumination. The contaminated water has a strong absorption peak around 465 or 663 nm due to the methyl orange (MO) or methylene blue (MB) absorption, respectively. After the solar treatment, the water contained no MO or MB, as evidenced by the near zero optical absorbance, showing an excellent sewage treatment performance. (c) Twenty-four hour (17 May 2017) continuous measurement of the solar flux and clean water generation. The ambient solar flux (red line), the quantity of the generated vapor (blue line) using open device, and condensed water (green line) using a covered device were recorded for one whole day (0:00–24:00).

monochromatic light are shown in Figure S12. Overall, the material works well under different wavelengths. A side-by-side comparison test with NIR and visible light indicated that the higher water production rates were obtained for NIR under the same condition (Figure 2c) due to the better thermal effect of NIR compared to that of visible light.<sup>7</sup> Furthermore, the production rates of water with 3DG under a microwave radiation of 2450 MHz at different power densities were also measured (Figure 2d and Figure S13; details in Supporting Information). As shown in Figure 2d, after irradiation of 4 min under 100 W, water with 3DG has a more than 3 times higher water evaporation than that without 3DG, indicating another efficient application scenario using microwave energy when sunlight is not available.

**Mechanism.** The thermal environment and heat transfer mechanism under light (10 sun) is analyzed in Figure 3a, and it involves several processes, including radiative (~4.4%) and convective (~2.9%) heat loss to the ambient and conductive (~2.7%) heat loss to the underlying water (detailed calculation shown in Supporting Information). A zoomed-in diagram is illuminated in Figure 3b to analyze the microscopic thermal environment. First, the combination of the intrinsic wide range and strong absorption of an individual graphene sheet with the cumulative effect due to the honeycomb multiple-layer stacked morphology ensures an efficient and broad absorption in the entire sunlight wavelength range all the way to the microwave.<sup>43</sup> Then, the absorbed solar energy by 3DG would

efficiently exchange the thermal energy with water saturated within the porosity of the material to generate the water vapor. Note that the hydrophilicity and porous structure cause an automatic water transport from the bulk water around into the sample. Furthermore, the ultralow density and low thermal conductivity make such a material work as a standalone solar thermal converter without the need for any extra insulator and effectively prevent the heat conduction to the underlying and surrounding water.

**Modeling.** As discussed above, the efficiency and specific water production rate are important in the practical application. So modeling was carried out to predict the ideal performance as well as to find the relationship of efficiency with the sample thickness. For an absorber, the efficient broadband absorption is a key factor for the solar thermal conversion efficiency. Based on the morphology analysis above, a structural model of a cube composed of single-layer graphene is built as the modeling unit (inset of Figure 3c) to show the relationship of absorption with the sample thickness (Figure S14; details in Supporting Information). Then an isothermal model is used to demonstrate the relationship between the efficiency and thickness of the 3DG (details in Supporting Information). The theoretical results agrees well with the experimental data (Figure 3c), showing that the efficiency of the 3DG material increases with the increased thickness, and the best experimental performance was achieved for 500 μm with a specific water evaporation rate of 2.6 kg m<sup>-2</sup> h<sup>-1</sup> g<sup>-1</sup>.

**Demo Application.** As shown in Figure S15, a practical device was set up for the desalination and sewage treatment. The 3DG material and salt (waste) water were placed at the center of the chamber. The steam was generated under the irradiation and then condensed into liquid when it arrived at the cold condenser. The condensed water automatically flowed along the container glass surfaces into the condensing receptacle under gravity (Movie S3). A saline water with four primary ions ( $\text{Na}^+$ ,  $\text{K}^+$ ,  $\text{Ca}^{2+}$ , and  $\text{Mg}^{2+}$ ) was used for the desalination. As can be seen from Figure 4a, after desalination, all the ions show 4 orders of ionic concentration decrement (Table S2), indicating an outstanding result better than that using industrial SWRO.<sup>9</sup> Meanwhile, the effect of sewage treatment was examined in the same way, and the quality of the generated clean water was verified using optical absorption spectra, which shows that the water contained negligible contaminant as evidenced by the near zero optical absorbance (Figure 4b).

**Outdoor Experiment.** Similar experiment was carried out using a large-scale device (15 cm in diameter) with 3DG (~170 mg) and natural sunlight outdoors for one whole day (0:00–24:00, 17 May 2017) to assess the real performance under the real factors such as varying solar flux and incident angles. The red line in Figure 4c shows the solar flux on a typical sunny day, and it reached the maximum from 10:00 to 15:00 of  $\sim 550 \text{ W m}^{-2}$  (0.55 sun, 38 °C). The 24 h continuous measurement was accomplished using both open (Figure S16) and covered (Figure S17) devices for comparison, and the quantity of the generated vapor (blue line) and water (green line) was recorded. Strikingly, the open and covered device achieved a high clean water generation of 8.84 and 6.97 kg per square meter all day, respectively. These results demonstrate its super sunlight capture and conversion ability to generate water under real and natural solar flux scenarios.

## CONCLUSIONS

In summary, we have demonstrated that a simple sheet of standalone graphene foam can act as efficient solar thermal capture and conversion device. The 3DG material can be used directly in an easy and scalable manner as a clean water generator with high efficiency under normal (1 sun) and even weaker sunlight (down to 0.25 sun). Furthermore, different from other desalination materials, our lightweight and elastic material is also highly portable for point of use and would be ideal for both personal and industrial application. This easy-to-use carbon material could provide many possibilities for high efficient solar energy harvesting and application opportunities for simplified water treatment.

## EXPERIMENTAL SECTION

**Synthesis of the 3D Graphene Material.** The starting material, graphene oxide, was synthesized by the oxidation of natural graphite powder using a modified Hummers' method based on references published elsewhere.<sup>40–42</sup> Three dimensionally cross-linked graphene, denoted as 3DG, was prepared following our previous procedures. A GO ethanol solution (30 mL,  $0.5 \text{ mg mL}^{-1}$ ) was sealed in a 50 mL Teflon-lined autoclave and heated to 180 °C and maintained at this temperature for 12 h. The autoclave was then naturally cooled to room temperature. Then the as-prepared ethanol-filled intermediate product was carefully removed from the autoclave to have a slow and gradual solvent exchange with water. After the solvent exchange process was totally completed, the water-filled product was freeze-dried and then dried in a vacuum oven at 100 °C for 2 h. Then the sample was annealed at 800 °C for 1 h in  $\text{H}_2/\text{Ar}$  mixture gas (5/95, v/v). Finally,

the sample was treated in a UV ozone system for 15 min to obtain the final graphene material (3DG).<sup>42</sup>

**Solar Vapor Generation Experiment.** 3DG materials of 15 mm in diameter were floating on the interface of the water/air with thicknesses from 150 to 2000  $\mu\text{m}$ , which were easily obtained using a laser (450 nm, 2 W) cutting. The solar beam from a solar simulator (7ILX500P, SOFN Instruments Co., LTD) was illuminated on the surface of the sample, and the weight loss was recorded. The temperature was measured using an IR camera (Fluke TiS65), and temperature probe and the weight change from evaporation were measured using an electronic mass balance (OHAUS, AX224ZH) with an accuracy of 0.1 mg. The evaporation mass loss of the receiver under dark conditions was measured and subtracted from the measured mass loss under solar illumination.

## ASSOCIATED CONTENT

### Supporting Information

The Supporting Information is available free of charge on the ACS Publications website at DOI: 10.1021/acsnano.7b08196.

Detailed experimental procedures, including the heat loss calculation, modeling, additional supplementary figures, and movie captions (PDF)

Movie S1 (AVI)

Movie S2 (AVI)

Movie S3 (AVI)

Movie S4 (AVI)

## AUTHOR INFORMATION

### Corresponding Author

\*E-mail: [yschen99@nankai.edu.cn](mailto:yschen99@nankai.edu.cn).

### ORCID

Yongsheng Chen: 0000-0003-1448-8177

### Notes

The authors declare no competing financial interest.

## ACKNOWLEDGMENTS

The authors gratefully acknowledge the financial support from Ministry of Science and Technology of China (MoST, 2016YFA0200200), the National Natural Science Foundation of China (NSFC, 21421001, 51633002, and 51472124), 111 Project (B12015), and Tianjin city (16ZXCLGX00100). The authors thank George Ni, Yanfei Xu, and Gang Chen (Massachusetts Institute of Technology) for helpful suggestions of the manuscript.

## REFERENCES

- (1) Lewis, N. S. Research Opportunities to Advance Solar Energy Utilization. *Science* **2016**, *351*, aad1920.
- (2) Lewis, N. S. Toward Cost-Effective Solar Energy Use. *Science* **2007**, *315*, 798–801.
- (3) Yu, G.; Gao, J.; Hummelen, J. C.; Wudl, F.; Heeger, A. J. Polymer Photovoltaic Cells: Enhanced Efficiencies via a Network of Internal Donor-Acceptor Heterojunctions. *Science* **1995**, *270*, 1789–1791.
- (4) Bach, U.; Lupo, D.; Comte, P.; Moser, J. E.; Weissortel, F.; Salbeck, J.; Spreitzer, H.; Gratzel, M. Solid-State Dye-Sensitized Mesoporous  $\text{TiO}_2$  Solar Cells with High Photon-to-Electron Conversion Efficiencies. *Nature* **1998**, *395*, 583–585.
- (5) Zou, Z. G.; Ye, J. H.; Sayama, K.; Arakawa, H. Direct Splitting of Water under Visible Light Irradiation with an Oxide Semiconductor Photocatalyst. *Nature* **2001**, *414*, 625–627.
- (6) Lu, Y.; Yang, Y.; Zhang, T.; Ge, Z.; Chang, H.; Xiao, P.; Xie, Y.; Hua, L.; Li, Q.; Li, H.; et al. Photoprompted Hot Electrons from Bulk Cross-Linked Graphene Materials and Their Efficient Catalysis for Atmospheric Ammonia Synthesis. *ACS Nano* **2016**, *10*, 10507–10515.

- (7) Ghasemi, H.; Ni, G.; Marconnet, A. M.; Loomis, J.; Yerci, S.; Miljkovic, N.; Chen, G. Solar Steam Generation by Heat Localization. *Nat. Commun.* **2014**, *5*, 4449.
- (8) Ni, G.; Li, G.; Boriskina, S. V.; Li, H.; Yang, W.; Zhang, T.; Chen, G. Steam Generation under One Sun Enabled by a Floating Structure with Thermal Concentration. *Nat. Energy* **2016**, *1*, 16126.
- (9) Zhou, L.; Tan, Y.; Wang, J.; Xu, W.; Yuan, Y.; Cai, W.; Zhu, S.; Zhu, J. 3D Self-Assembly of Aluminium Nanoparticles for Plasmon-Enhanced Solar Desalination. *Nat. Photonics* **2016**, *10*, 393–398.
- (10) Hu, X.; Xu, W.; Zhou, L.; Tan, Y.; Wang, Y.; Zhu, S.; Zhu, J. Tailoring Graphene Oxide-Based Aerogels for Efficient Solar Steam Generation under One Sun. *Adv. Mater.* **2017**, *29*, 1604031.
- (11) Ito, Y.; Tanabe, Y.; Han, J.; Fujita, T.; Tanigaki, K.; Chen, M. Multifunctional Porous Graphene for High-Efficiency Steam Generation by Heat Localization. *Adv. Mater.* **2015**, *27*, 4302–4307.
- (12) Liu, Y.; Yu, S.; Feng, R.; Bernard, A.; Liu, Y.; Zhang, Y.; Duan, H.; Shang, W.; Tao, P.; Song, C.; et al. A Bioinspired, Reusable, Paper-Based System for High-Performance Large-Scale Evaporation. *Adv. Mater.* **2015**, *27*, 2768–2774.
- (13) Zhang, L.; Tang, B.; Wu, J.; Li, R.; Wang, P. Hydrophobic Light-to-Heat Conversion Membranes with Self-Healing Ability for Interfacial Solar Heating. *Adv. Mater.* **2015**, *27*, 4889–4894.
- (14) Shannon, M. A.; Bohn, P. W.; Elimelech, M.; Georgiadis, J. G.; Mariñas, B. J.; Mayes, A. M. Science and Technology for Water Purification in the Coming Decades. *Nature* **2008**, *452*, 301–310.
- (15) Elimelech, M.; Phillip, W. A. The Future of Seawater Desalination: Energy, Technology, and the Environment. *Science* **2011**, *333*, 712–717.
- (16) Wang, L.; Boutilier, M. S. H.; Kidambi, P. R.; Jang, D.; Hadjiconstantinou, N. G.; Karnik, R. Fundamental Transport Mechanisms, Fabrication and Potential Applications of Nanoporous Atomically Thin Membranes. *Nat. Nanotechnol.* **2017**, *12*, 509–522.
- (17) Cohen-Tanugi, D.; Grossman, J. C. Nanoporous Graphene as a Reverse Osmosis Membrane: Recent Insights from Theory and Simulation. *Desalination* **2015**, *366*, 59–70.
- (18) Malaeb, L.; Ayoub, G. M. Reverse Osmosis Technology for Water Treatment: State of the Art Review. *Desalination* **2011**, *267*, 1–8.
- (19) Lee, K. P.; Arnot, T. C.; Mattia, D. A Review of Reverse Osmosis Membrane Materials for Desalination-Development to Date and Future Potential. *J. Membr. Sci.* **2011**, *370*, 1–22.
- (20) Fritzmann, C.; Loewenberg, J.; Wintgens, T.; Melin, T. State-of-The-Art of Reverse Osmosis Desalination. *Desalination* **2007**, *216*, 1–76.
- (21) Liu, Z.; Song, H.; Ji, D.; Li, C.; Cheney, A.; Liu, Y.; Zhang, N.; Zeng, X.; Chen, B.; Gao, J.; et al. Extremely Cost-Effective and Efficient Solar Vapor Generation under Nonconcentrated Illumination Using Thermally Isolated Black Paper. *Global Challenges* **2017**, *1*, 1600003.
- (22) Jiang, Q.; Tian, L.; Liu, K.-K.; Tadepalli, S.; Raliya, R.; Biswas, P.; Naik, R. R.; Singamaneni, S. Bilayered Biofoam for Highly Efficient Solar Steam Generation. *Adv. Mater.* **2016**, *28*, 9400–9407.
- (23) Wang, J.; Li, Y.; Deng, L.; Wei, N.; Weng, Y.; Dong, S.; Qi, D.; Qiu, J.; Chen, X.; Wu, T. High-Performance Photothermal Conversion of Narrow-Bandgap  $\text{Ti}_2\text{O}_3$  Nanoparticles. *Adv. Mater.* **2017**, *29*, 1603730.
- (24) Richardson, H. H.; Hickman, Z. N.; Govorov, A. O.; Thomas, A. C.; Zhang, W.; Kordesch, M. E. Thermo-optical Properties of Gold Nanoparticles Embedded in Ice: Characterization of Heat Generation and Melting. *Nano Lett.* **2006**, *6*, 783–788.
- (25) Zhou, L.; Tan, Y.; Ji, D.; Zhu, B.; Zhang, P.; Xu, J.; Gan, Q.; Yu, Z.; Zhu, J. Self-Assembly of Highly Efficient, Broadband Plasmonic Absorbers for Solar Steam Generation. *Sci. Adv.* **2016**, *2*, e1501227.
- (26) Bae, K.; Kang, G.; Cho, S. K.; Park, W.; Kim, K.; Padilla, W. J. Flexible Thin-Film Black Gold Membranes with Ultrabroadband Plasmonic Nanofocusing for Efficient Solar Vapour Generation. *Nat. Commun.* **2015**, *6*, 10103.
- (27) Zhou, L.; Zhuang, S.; He, C.; Tan, Y.; Wang, Z.; Zhu, J. Self-Assembled Spectrum Selective Plasmonic Absorbers with Tunable Bandwidth for Solar Energy Conversion. *Nano Energy* **2017**, *32*, 195–200.
- (28) Liu, Y.; Lou, J.; Ni, M.; Song, C.; Wu, J.; Dasgupta, N. P.; Tao, P.; Shang, W.; Deng, T. Bioinspired Bifunctional Membrane for Efficient Clean Water Generation. *ACS Appl. Mater. Interfaces* **2016**, *8*, 772–779.
- (29) Wang, X.; Ou, G.; Wang, N.; Wu, H. Graphene-Based Recyclable Photo-Absorbers for High-Efficiency Seawater Desalination. *ACS Appl. Mater. Interfaces* **2016**, *8*, 9194–9199.
- (30) Jin, H. C.; Lin, G. P.; Bai, L. Z.; Zeiny, A.; Wen, D. S. Steam Generation in a Nanoparticle-Based Solar Receiver. *Nano Energy* **2016**, *28*, 397–406.
- (31) Zhao, D.; Duan, H.; Yu, S.; Zhang, Y.; He, J.; Quan, X.; Tao, P.; Shang, W.; Wu, J.; Song, C.; et al. Enhancing Localized Evaporation through Separated Light Absorbing Centers and Scattering Centers. *Sci. Rep.* **2015**, *5*, 17276.
- (32) Zeng, Y.; Yao, J.; Horri, B. A.; Wang, K.; Wu, Y.; Li, D.; Wang, H. Solar Evaporation Enhancement Using Floating Light-Absorbing Magnetic Particles. *Energy Environ. Sci.* **2011**, *4*, 4074–4078.
- (33) Li, X.; Xu, W.; Tang, M.; Zhou, L.; Zhang, B.; Zhu, S.; Zhu, J. Graphene Oxide-Based Efficient and Scalable Solar Desalination under One Sun with a Confined 2D Water Path. *Proc. Natl. Acad. Sci. U. S. A.* **2016**, *113*, 13953–13958.
- (34) Li, Y.; Gao, T.; Yang, Z.; Chen, C.; Luo, W.; Song, J.; Hitz, E.; Jia, C.; Zhou, Y.; Liu, B.; et al. 3D-Printed, All-in-One Evaporator for High-Efficiency Solar Steam Generation under 1 Sun Illumination. *Adv. Mater.* **2017**, *29*, 1700981.
- (35) Zhang, P.; Li, J.; Lv, L.; Zhao, Y.; Qu, L. Vertically Aligned Graphene Sheets Membrane for Highly Efficient Solar Thermal Generation of Clean Water. *ACS Nano* **2017**, *11*, 5087–5093.
- (36) Liu, K.-K.; Jiang, Q.; Tadepalli, S.; Raliya, R.; Biswas, P.; Naik, R. R.; Singamaneni, S. Wood–Graphene Oxide Composite for Highly Efficient Solar Steam Generation and Desalination. *ACS Appl. Mater. Interfaces* **2017**, *9*, 7675–7681.
- (37) Xu, N.; Hu, X.; Xu, W.; Li, X.; Zhou, L.; Zhu, S.; Zhu, J. Mushrooms as Efficient Solar Steam-Generation Devices. *Adv. Mater.* **2017**, *29*, 1606762.
- (38) Li, X.; Lin, R.; Ni, G.; Xu, N.; Hu, X.; Zhu, B.; Lv, G.; Li, J.; Zhu, S.; Zhu, J. Three-Dimensional Artificial Transpiration for Efficient Solar Waste-Water Treatment. *Natl. Sci. Rev.* **2017**, DOI: 10.1093/nsr/nwx051.
- (39) Ren, H.; Tang, M.; Guan, B.; Wang, K.; Yang, J.; Wang, F.; Wang, M.; Shan, J.; Chen, Z.; Wei, D.; et al. Hierarchical Graphene Foam for Efficient Omnidirectional Solar–Thermal Energy Conversion. *Adv. Mater.* **2017**, *29*, 1702590.
- (40) Wu, Y.; Yi, N.; Huang, L.; Zhang, T.; Fang, S.; Chang, H.; Li, N.; Oh, J.; Lee, J. A.; Kozlov, M.; et al. Three-Dimensionally Bonded Spongy Graphene Material with Super Compressive Elasticity and Near-Zero Poisson's Ratio. *Nat. Commun.* **2015**, *6*, 6141.
- (41) Zhang, T. F.; Chang, H. C.; Wu, Y. P.; Xiao, P. S.; Yi, N. B.; Lu, Y. H.; Ma, Y. F.; Huang, Y.; Zhao, K.; Yan, X. Q.; et al. Macroscopic and Direct Light Propulsion of Bulk Graphene Material. *Nat. Photonics* **2015**, *9*, 471–476.
- (42) Chang, H.; Qin, J.; Xiao, P.; Yang, Y.; Zhang, T.; Ma, Y.; Huang, Y.; Chen, Y. Highly Reversible and Recyclable Absorption under Both Hydrophobic and Hydrophilic Conditions Using a Reduced Bulk Graphene Oxide Material. *Adv. Mater.* **2016**, *28*, 3504–3509.
- (43) Zhang, Y.; Huang, Y.; Zhang, T.; Chang, H.; Xiao, P.; Chen, H.; Huang, Z.; Chen, Y. Broadband and Tunable High-Performance Microwave Absorption of an Ultralight and Highly Compressible Graphene Foam. *Adv. Mater.* **2015**, *27*, 2049–2053.